


Cite this: *RSC Adv.*, 2020, 10, 7328

# Selective recovery of zinc from goethite residue in the zinc industry using deep-eutectic solvents†

Nerea Rodriguez Rodriguez, <sup>\*,ab</sup> Lieven Machiels,<sup>a</sup> Bieke Onghena, <sup>a</sup>  
Jeroen Spooren <sup>c</sup> and Koen Binnemans <sup>a</sup>

Several deep-eutectic solvents (DESs) were tested for the valorisation of goethite residue produced by the zinc industry. The objective of the work was to selectively recover zinc from the iron-rich matrix using deep-eutectic solvents as lixiviants. The effect of the type of hydrogen bond donor and hydrogen bond acceptor of the deep-eutectic solvent on the leaching efficiency was studied. Levulinic acid–choline chloride ( $x_{\text{ChCl}} = 0.33$ ) (LevA–ChCl) could selectively leach zinc from the iron-rich matrix, and it was selected as the best-performing system to be used in further study. The leaching process was optimised in terms of temperature, contact time, liquid-to-solid ratio and water content of the deep-eutectic solvent. The role of the choline cation on the leaching process was investigated by considering the leaching properties of a LevA–CaCl<sub>2</sub> mixture. The goethite residue was also leached with pure levulinic acid. The results were compared to a purely hydrometallurgical approach using sulphuric acid leaching. Leaching with LevA–ChCl resulted in higher selectivity compared to the conventional “hot leaching” with 80 g L<sup>−1</sup> sulphuric acid. Furthermore, a slightly higher zinc recovery and comparable selectivity for zinc over iron were achieved with LevA–ChCl compared to conventional “neutral leaching” with 10 g L<sup>−1</sup> sulphuric acid.

Received 10th January 2020  
Accepted 10th February 2020

DOI: 10.1039/d0ra00277a

rsc.li/rsc-advances

## Introduction

The mining and metal processing industry has been landfilling and/or stockpiling vast quantities of metal-containing residues. In the long term, tailing ponds and industrial landfills may represent an environmental and health liability. The presence of (easily) accessible base and critical metals make these wastes a potential secondary source of metals. The development of sustainable processes for near-zero-waste metal production are required for the implementation of a global circular economy. Besides, this could also mitigate the restricted access of Europe to ore deposits.<sup>1,2</sup>

More than 95% of the global zinc production is obtained *via* the roasting–leaching–electrowinning (RLE) process.<sup>3</sup> In this process, a zinc sulphide concentrate, (Zn, Fe)S, is roasted to calcine, from which zinc is leached with sulphuric acid (H<sub>2</sub>SO<sub>4</sub>) and recovered from the pregnant leach solution (PLS) *via* electrowinning. The first leaching step is the so-called “neutral leaching” (60–80 °C, 10 g L<sup>−1</sup> H<sub>2</sub>SO<sub>4</sub>), which is very selective against iron. The PLS of the neutral leaching is fed directly into

the electrowinning step. The second leaching step is the so-called “hot leaching” (≈100 °C, 30–80 g L<sup>−1</sup> H<sub>2</sub>SO<sub>4</sub>), which solubilizes most of the remaining zinc and the majority of the iron. As the presence of iron ions in the PLS would hinder the downstream zinc electrodeposition, the PLS of the hot leaching is purified before the electrowinning by precipitation of the iron.<sup>3</sup> The form in which the iron is precipitated names the entire process: the jarosite, the goethite or the hematite process. The iron-rich precipitate is the largest residual stream, namely, 0.4 tons of jarosite per ton of ore, or 0.25 tons of goethite per ton of ore.<sup>4</sup> The goethite process produces less residue than the jarosite process, *ca.* 75%, but the zinc losses are higher (8–10%) compared to the jarosite process (3–5%).<sup>5</sup> In the goethite process the iron is precipitated in the trivalent form as goethite (FeO(OH)). Firstly, the iron(III) is reduced to iron(II) using zinc sulphide concentrate, and then the pH is adjusted to pH 3.5–4 by addition of calcine and exposure to air resulting in the re-oxidation of iron(II) to iron(III).

The valorisation of the goethite residue has been the subject of various studies. Thermal processes based on plasma fuming, inorganic polymerization, or transformation into glass ceramic are the most commonly reported.<sup>4,6–12</sup> However, life cycle assessment studies showed that due to the high energy consumption, the environmental impact of valorisation is similar to that of landfilling.<sup>13</sup> Hydrometallurgical processes are more commonly reported for the valorisation of jarosite<sup>14–19</sup> than for that of goethite.<sup>20</sup>

<sup>a</sup>Department of Chemistry, KU Leuven, Celestijnenlaan 200F, P. O. Box 2404, B-3001 Leuven, Belgium. E-mail: nerea.rodriguezrodriguez@kuleuven.be

<sup>b</sup>SIM vzw, Technologiepark 935, B-9052 Zwijnaarde, Belgium

<sup>c</sup>Waste Recycling Technologies, Sustainable Materials Management, Flemish Institute for Technological Research, VITO N.V., Boeretang 200, 2400 Mol, Belgium

† Electronic supplementary information (ESI) available: XRD and EPMA of the goethite residue. Composition of PLSs. See DOI: 10.1039/d0ra00277a



In this work, a new solvometallurgical approach is proposed to selectively recover zinc from goethite residue. Solvometallurgy is a new branch of extractive metallurgy that uses non-aqueous solvents such as molecular organic solvents, ionic liquids or deep-eutectic solvents instead of aqueous solutions.<sup>21</sup> Solvometallurgy is less energy intensive than pyrometallurgy, and it has shown better selectivity than hydrometallurgy in the valorisation of other residues, including jarosite residue in the zinc industry.<sup>22–26</sup> Deep-eutectic solvents (DESs) are defined as a mixture of pure compounds, generally a hydrogen bond donor (HBD) and a hydrogen bond acceptor (HBA), for which the eutectic point temperature is below that of an ideal liquid mixture.<sup>27–29</sup> DESs have been previously used as lixiviants for the solubilization of different metals.<sup>30–32</sup> This work focusses on the selection of DESs for the selective leaching of zinc against iron for the valorisation of the goethite residue, optimization of the leaching process, and critical assessment of the obtained results. DESs have already proven to be suitable for the selective extraction of zinc over iron from electric arc furnace dust.<sup>33</sup>

## Experimental

### Chemicals

Choline chloride (99%), ethylene glycol (99.5%), urea (99.5%) and Triton X-10 were purchased from Acros Organics NV (Geel, Belgium). Levulinic acid (99%) was purchased from J&K Scientific BVBA (Pforzheim, Germany). Tetrabutylammonium chloride (97 wt%) was purchased from Sigma Aldrich (Steinheim, Germany). Tetrabutylphosphonium chloride (>95 wt%) was obtained from Io-Li-Tec (Heilbronn, Germany). Nitric acid, HNO<sub>3</sub>, (>65%) and anhydrous calcium chloride, CaCl<sub>2</sub>, (>95%) were purchased from Chem-Lab NV (Zedelgem, Belgium). Hydrochloric acid, HCl, (>37%) was purchased from VWR (Fontenay-sous-Bois, France). A silicon solution in isopropanol was purchased from SERVA Electrophoresis GmbH (Heidelberg, Germany). The standard solutions (1000 µg mL<sup>-1</sup>) of zinc, iron, copper, lead, calcium, arsenic, lutetium, niobium and platinum were purchased from Chem-Lab (Zedelgem, Belgium). Water was always of ultrapure quality, deionized to a resistivity of 18.2 MΩ cm with a Millipore Reference+ ultrapure water system. All chemicals were used as received without any further purification. The goethite residue was kindly provided by Nyrstar (Balen, Belgium).

### Instrumentation

The material was ground and sieved using a mortar grinder (Fritsch, Pulverisette 2) and a vibratory sieve shaker (Fritsch, Analysette 3). The goethite was digested using a microwave digester (8 positions, Milestone). The metal content of the digested samples was measured *via* inductively coupled plasma optical emission spectroscopy (ICP-OES), Optima 3000DV from PerkinElmer. The metal content of all the PLSs was determined *via* ICP-OES, Optima 8300 from PerkinElmer, with the exception of the screening experiments for DES selection, where the metal content of the different samples was measured using a portable benchtop Bruker Total Reflection X-ray Fluorescence (TXRF)

Spectrometer S2 Picofox. An Eppendorf 5804 centrifuge was used to facilitate the phase separation. X-ray powder diffraction (XRD) was used for the phase identification of the crystalline fraction (Bruker D2 Phaser). The quantitative XRDs were performed with a PANalytical EMPYREAN system operated at 40 kV and 45 mA, with a cobalt anode and equipped with a BBHD (Bragg Brentano High Definition) and a 3D detector (PIXcel 3D) with an active scanning length of 3.347° 2θ. The water content of the DESs was measured using a Mettler-Toledo V30S KF titrator where HYDRANAL™ – Composite 5, and HYDRANAL™ – Methanol dry (Honeywell, Fluka) were used as titrant and medium, respectively.

### Procedure

The material was dried in a ventilated oven at 40 °C until no mass changes were detected, and then it was ground (gap 0, 10 min) and sieved (1 mm pore size mesh). For the elemental analysis, about 0.5 g of sample was weighed into the digestion vessels. Then, the following acids were added: 4 mL HCl, 3 mL HNO<sub>3</sub> and 1 mL HBF<sub>4</sub>. The digestion vessels were placed into the microwave unit and the following digestion process was applied: 2 min at 250 W, 2 min at 0 W, 5 min at 250 W, 5 min at 400 W and 5 min at 500 W. At the end of the programme the vessels were cooled down to room temperature. Subsequently, 22 mL of 4 wt% of H<sub>3</sub>BO<sub>3</sub> was added and the vessels were placed again in the microwave unit applying the following process: 3 min, 300 W. After cooling, the digested solution were transferred to volumetric flasks and filled up to 100 mL with ultrapure water for analysis.

For the standard XRD measurements the following parameters were applied: 2θ = 20–90°, radiation = CuK<sub>α</sub>, acceleration voltage = 40 kV, acceleration current = 40 mA, a step size of 0.020° and a counting time of 1 s per step, spin mode. The X'Pert HighScore software was used to analyse the collected data by comparison with the ICDD (International Centre for Diffraction Data). Quantitative analyses by Rietveld refinement used an external standard (TiO<sub>2</sub>, Kronos International) as reference measurement. Continuous mode scans with a scanning speed of 0.06° s<sup>-1</sup> and step size of 0.013° were performed within a 2θ range of 5–120°. The obtained diffractograms were quantitatively analysed with HighScore Plus software.

The DESs were prepared *via* the heating method: the components were placed together in closed vials, and heated (60 °C) while stirring (500 rpm) using a magnetic stirrer with a temperature controller until a clear liquid was formed. The water content of the freshly prepared DESs was measured *via* Karl Fischer titration. DESs with different water contents were prepared by adding the required amount of water.

For the DES selection, small scale (1 mL) leaching experiments were performed. The goethite and the DES were mixed in a microcentrifuge tube and mixed at 40 °C for 48 h using an Eppendorf Thermomixer® C. Thereafter, the samples were filtered using syringe filters with pore size of 0.45 µm. The metal concentration was measured *via* TXRF. The optimization of the analytical procedure has been described in a previous paper.<sup>34</sup> Briefly, the samples were diluted 20 times in a Triton X-100



solution (10 wt% in water) and lutetium was added as internal standard. Silicone solution SERVA (30  $\mu\text{L}$ ) was added on the carrier surface and dried for 5 min at 80  $^{\circ}\text{C}$  in a hot air oven. A small droplet (3  $\mu\text{L}$ ) of the diluted sample was added onto the hydrophobized carrier. Then, the carrier was dried in a hot air oven for 30 min at 80  $^{\circ}\text{C}$ .

After DES selection, the rest of leaching experiments were performed on a larger scale: 0.5 to 1 g of material was placed in a 15 mL Eppendorf tube, the lixiviant was added, and the closed vial was mixed using an Eppendorf ThermoMixer C. After the leaching, the samples were centrifuged (4000 rpm, 5 min) and filtered using PET syringe filters (pore size 0.45  $\mu\text{m}$ ). The metal content of the samples was measured *via* ICP-OES. The samples were 10 or 100 times diluted with 2 vol%  $\text{HNO}_3$  to have a final metal concentration lower than 50 ppm. Niobium (5 ppm) and platinum (5 ppm) were added as internal standard. All the leaching experiments were performed in duplicate.

## Results and discussion

### Material characterization

The goethite sludge was dried, grounded and sieved, and only the fraction smaller than 1 mm was used in this study. The results of the elemental analysis show that the material is mainly composed of iron (24.1 wt%), zinc (5.9 wt%) and calcium (5.5 wt%), lead (1.8 wt%) and copper (0.4 wt%). The XRD analysis (Fig. 1) shows that, in the crystalline fraction, iron is present in magnetite, franklinite and jarosite mineral phases, whereas zinc is mostly present in the form of franklinite and willemite. No crystalline goethite phase was observed and is expected to be part of the amorphous phase. The XRD pattern is included in the ESI, Fig. S1.†

### Selection of DES

The ability of different DESs to leach goethite was evaluated. The selected DESs were: urea–choline chloride ( $x_{\text{ChCl}} = 0.33$ ) (urea–ChCl), ethylene glycol–choline chloride ( $x_{\text{ChCl}} = 0.33$ ) (EtGly–ChCl), levulinic acid–choline chloride ( $x_{\text{ChCl}} = 0.33$ ) (LevA–ChCl), levulinic acid–tetrabutylammonium chloride ( $x_{\text{TbaCl}} = 0.33$ ) (LevA–TbaCl), and levulinic acid–tetrabutylphosphonium chloride ( $x_{\text{TbpCl}} = 0.33$ ) (LevA–TbpCl). Within this selection, the most commonly used HBDs (amides, polyols,

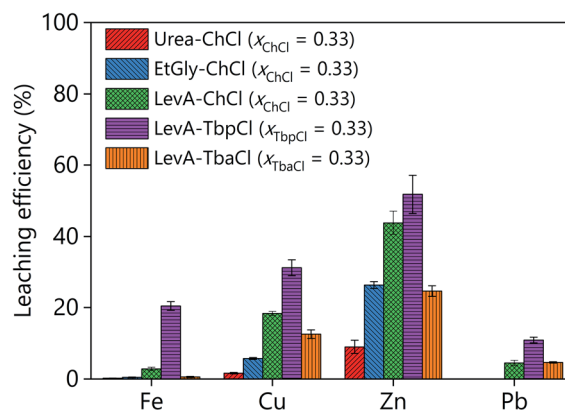


Fig. 2 Leaching efficiency of the goethite residue using different DESs as lixiviant. The experimental conditions were:  $L/S = 10$ ;  $T = 40\text{ }^{\circ}\text{C}$ ; and  $t = 24\text{ h}$ .

and carboxylic acids) and HBAs (symmetric quaternary ammonium and phosphonium salts, and asymmetric quaternary ammonium salts) were considered. For the first screening tests, the DESs were used to leach goethite under moderate conditions (liquid-to-solid ratio ( $L/S$ ) = 10;  $T = 40\text{ }^{\circ}\text{C}$ ; and  $t = 24\text{ h}$ ). The results show that the leaching efficiency of zinc increased in the following order: urea–ChCl < EtGly–ChCl < LevA–ChCl (Fig. 2). The leaching efficiency of other metals such as iron, copper and lead followed the same trend. These results are in agreement with literature data, where higher metal oxide solubilities were reported for DESs containing acidic HBDs like levulinic acid, compared to those containing amides and polyols, like urea and ethylene glycol.<sup>30,32</sup> Furthermore, for the DESs with the same HBD the leaching efficiency of zinc and iron increased in the following order: LevA–TbaCl < LevA–ChCl < LevA–TbpCl. The increase in the size of the central atom of the quaternary salt drastically increased the solubility of all the metals. This behaviour could be attributed to the weaker intramolecular interactions in the DES due to the lower electronegativity of the phosphonium cation, which could make both the levulinic acid and the tetrabutylphosphonium chloride more available for interaction with metals. To the best of our knowledge, this is the first time that the effect of the HBA on the solubility of metals is considered.

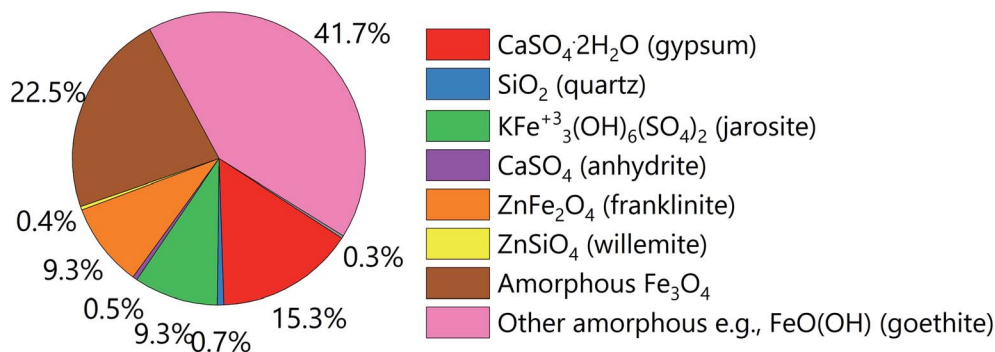


Fig. 1 Mineral phases identified *via* QXRD.



**Table 1** Composition of the pregnant leach solution obtained from the leaching of goethite residue using different DESs. The selectivity of zinc towards iron ( $\alpha$ ) is also included<sup>a</sup>

DES	Fe (mg L <sup>-1</sup> )	Cu (mg L <sup>-1</sup> )	Zn (mg L <sup>-1</sup> )	Pb (mg L <sup>-1</sup> )	$\alpha$
Urea–ChCl	55	7	532	0	10
EtGly–ChCl	115	25	1555	0	14
LevA–ChCl	731	84	2765	86	4
LevA–TbpCl	4957	134	3062	195	1
LevA–TbaCl	138	54	1453	83	11

<sup>a</sup> Leaching conditions: L/S = 10; T = 40 °C; and t = 24 h.

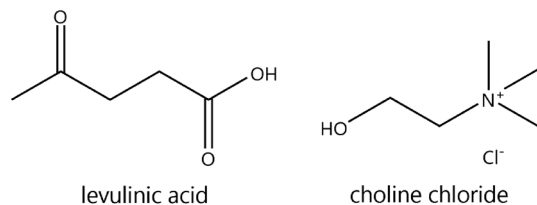


**Fig. 3** Chemical structure of the components of the DES.

The leaching efficiency of zinc was higher than the leaching efficiency of iron in all cases. Low solubility of Fe(III) was expected from previous literature.<sup>30</sup> Nonetheless, the concentration of iron in the PLS was higher than what has been previously reported in other works.<sup>33</sup> However, the iron mineralogy of the studied sample, containing mostly goethite/magnetite, differs from the samples in previous works that are rich in franklinite. Considering that the objective of this work is to selectively leach zinc from the iron-rich matrix, the selected DES should combine a high zinc leaching efficiency with a high selectivity against iron. Table 1 shows the composition of the pregnant leach solution and the selectivity ( $\alpha$ ) of zinc against iron, calculated according to eqn (1):

$$\alpha_{\text{Zn/Fe}} = \frac{C_{\text{Zn}}}{C_{\text{Fe}}} \quad (1)$$

where  $C_{\text{Zn}}$  is the concentration of zinc (mg L<sup>-1</sup>) and  $C_{\text{Fe}}$  is the concentration of iron (mg L<sup>-1</sup>) in the DES leachate. Urea–ChCl, EtGly–ChCl and LevA–TbpCl were found to be very selective against iron ( $\alpha \geq 10$ ), but the leaching efficiency of zinc was very low. LevA–TbpCl had the highest leaching efficiency of zinc, but it was the least selective against iron ( $\alpha = 1$ ). LevA–ChCl showed

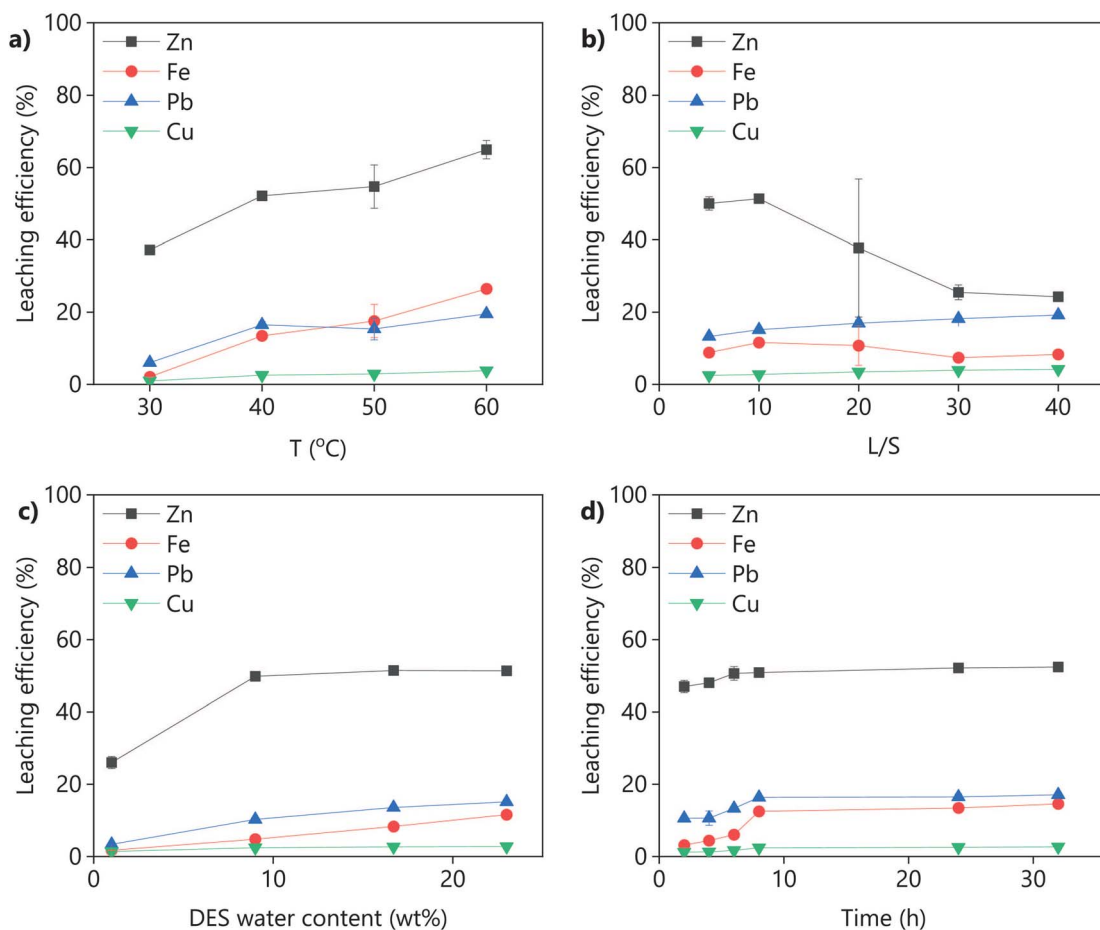


**Fig. 4** Effect on the LevA–ChCl leaching of goethite of (a) the temperature (L/S = 10; t = 24 h; H<sub>2</sub>O (wt%) = 30; 1000 rpm). (b) The L/S (T = 40 °C; t = 48 h; H<sub>2</sub>O (wt%) = 23; 1000 rpm). (c) The DES water content (T = 40 °C; t = 48 h; L/S = 10; 1000 rpm). (d) The leaching time (T = 40 °C; t = 24 h; H<sub>2</sub>O (wt%) = 30; 1000 rpm).





the best compromise between leaching efficiency of zinc and selectivity against iron ( $\alpha = 4$ ). Therefore, it was selected for the rest of the work. The molecular structure of the components of this DES are shown in Fig. 3.

### Optimization of the leaching process

The leaching of the goethite residue using LevA–ChCl was optimized in terms of temperature, water content of the DES, L/S ratio and leaching time. Increasing the leaching temperature increased the leachability of all the metals, but it decreased the selectivity (Fig. 4a, Table S1†). A temperature increase from 30 °C to 60 °C enhanced the zinc leaching efficiency from 37 to 65%, but decreased the selectivity of zinc against iron from 4.3 to 0.8. At the investigated conditions, only temperatures lower than 40 °C resulted in a selective zinc leaching ( $\alpha > 1$ ). Low L/S ratios ( $\leq 10$ ) improved both the zinc leaching efficiency and the selectivity (Fig. 4b, Table S2†). However, the high viscosity of the DES made the solid–liquid separation and mixing difficult for L/S lower than five. Increasing the water content of the DES increased the leaching efficiency of zinc but decreased its selectivity against iron (Fig. 4c and Table S3†). Pure LevA–ChCl ( $\approx 1$  wt% H<sub>2</sub>O) could leach 26 wt% of zinc, with a selectivity against iron close to four. When the water content of the DES was increased to 9 wt%, the amount of leached zinc was almost doubled, but the amount of leached iron was tripled. Further increase of the water content of the DES did not have any effect on the leaching of zinc, but it drastically increased the leaching of iron. A possible reason for that could be that the metals are better solvated by water, especially the iron. Although increasing the water content sacrificed selectivity, it also

reduced the viscosity of the DES which simplified both the mixing and the solid–liquid separation. For example, the viscosity of LevA–ChCl at 20 °C is 320 mPa s (H<sub>2</sub>O wt% = 0.5) and 53 mPa s (H<sub>2</sub>O wt% = 10).<sup>35</sup> Further upscaling and economic analysis would be required to solve this trade-off. The effect of the leaching time was also investigated (Fig. 4d, Table S4†), and it was observed that the difference in the leaching time can be exploited to favour the selectivity.

To gain more insight into the selectivity of the leaching system, the scatter plot matrix shown in Fig. 5 was constructed.<sup>36,37</sup> Each point represents the composition of the PLS obtained from a different leaching experiment. This type of graph allows to determine whether the leaching of the different metal pairs is correlated and if the correlation is positive or negative. The leaching of the zinc–lead, zinc–copper and copper–lead pairs are linearly correlated. Therefore, it is not possible to selectively leach those pairs with LevA–ChCl. The iron-containing pairs (iron–zinc, iron–lead and iron–copper) are positively, but not linearly correlated. The non-linearly correlated region corresponds to the leaching time optimization experiments. Unfortunately, this graph also shows that high selectivity cannot be achieved in combination with a high leaching efficiency of zinc by optimization of the leaching time.

### Role of choline cation in the leaching of goethite

To further understand the system, the role of the choline cation on the leaching was investigated: is the role of the cation only to act as a counter ion for the chloride, *i.e.* to give sufficiently high chloride concentration, or is there any synergistic effect when combined with levulinic acid? The results obtained using LevA–

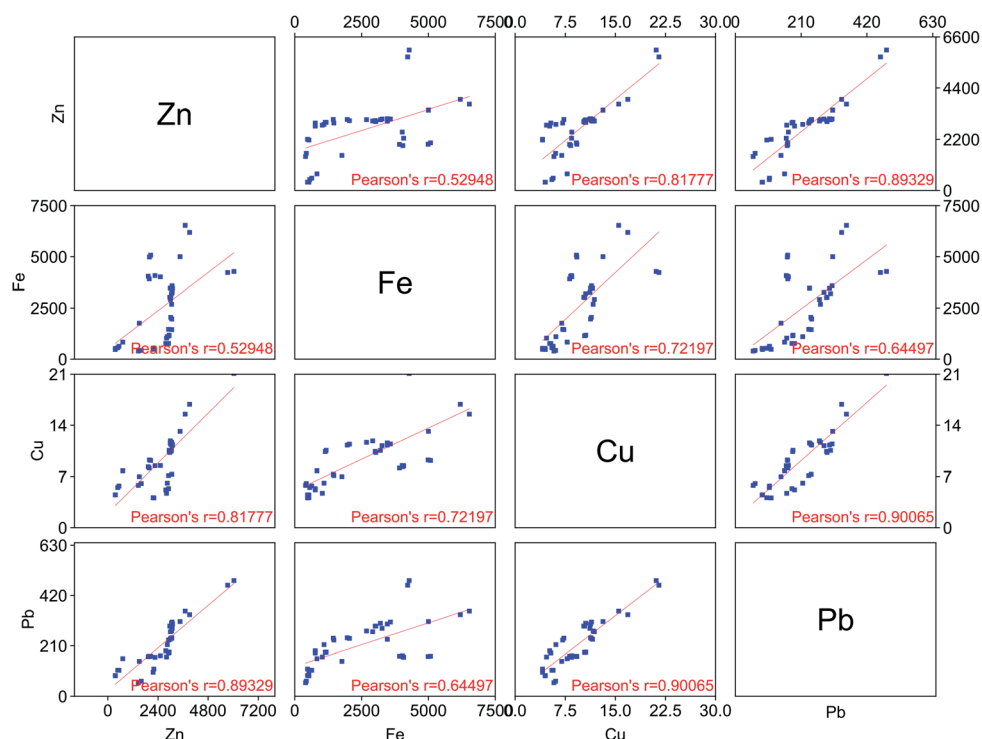


Fig. 5 Scatterplot for the composition of the pregnant leach solution (in ppm) using LevA–ChCl under different experimental conditions.



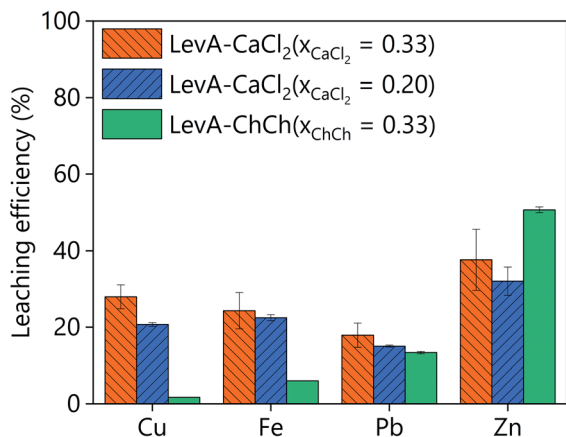


Fig. 6 Goethite leaching efficiency using LevA-ChCl ( $x_{\text{ChCl}} = 0.33$ ) (green), LevA-CaCl<sub>2</sub> ( $x_{\text{CaCl}_2} = 0.33$ ) (orange) and LevA-CaCl<sub>2</sub> ( $x_{\text{CaCl}_2} = 0.20$ ) (blue) at L/S = 10;  $t = 6$  h;  $T = 40$  °C; H<sub>2</sub>O wt% = 30.

ChCl ( $x_{\text{ChCl}} = 0.33$ ) were compared to those obtained using LevA-CaCl<sub>2</sub> ( $x_{\text{CaCl}_2} = 0.33$ ) under the same leaching conditions (Fig. 6). The experiments showed that the use of choline chloride instead of CaCl<sub>2</sub> increased both the leaching efficiency of zinc and the selectivity against iron and copper. The leaching of lead was not affected by the substitution of the choline chloride by CaCl<sub>2</sub>. This means that the choline cation plays an important

role in the solvation of the metal ion together with the chloride anions. Furthermore, an increase of the CaCl<sub>2</sub> concentration, *i.e.*, LevA-CaCl<sub>2</sub> ( $x_{\text{CaCl}_2} = 0.20$ ) vs. LevA-CaCl<sub>2</sub> ( $x_{\text{CaCl}_2} = 0.33$ ) increased the leaching efficiency of all the metals, but the effect was not very significant. It should be noticed that the composition of LevA-CaCl<sub>2</sub> ( $x_{\text{CaCl}_2} = 0.20$ ) was chosen to have the same proportion of chloride ions as LevA-ChCl ( $x_{\text{ChCl}} = 0.33$ ). This suggests that the concentration of chloride does not have a critical effect on the leaching efficiency.

Furthermore, the effect of different parameters (temperature, water content, leaching time, L/S ratio) on the leaching efficiency of goethite using LevA-CaCl<sub>2</sub> ( $x_{\text{CaCl}_2} = 0.33$ ) has been investigated. The obtained results have been plotted, together with those obtained for LevA-CaCl<sub>2</sub> ( $x_{\text{CaCl}_2} = 0.20$ ), in a scatter plot (Fig. 7). Contrarily to what has been shown in Fig. 5 for LevA-ChCl, all the metal pairs show a good linear positive correlation (see Pearson's  $r$  values). From the analysis of Fig. 5 and 7 it can be concluded that the presence of the choline cation can positively influence the selectivity of certain metal pairs.

### Role of choline chloride in the leaching of goethite

Pure levulinic acid was used to leach goethite and the obtained results were compared to those obtained using LevA-ChCl (Fig. 8). Under the same leaching conditions, the leaching of

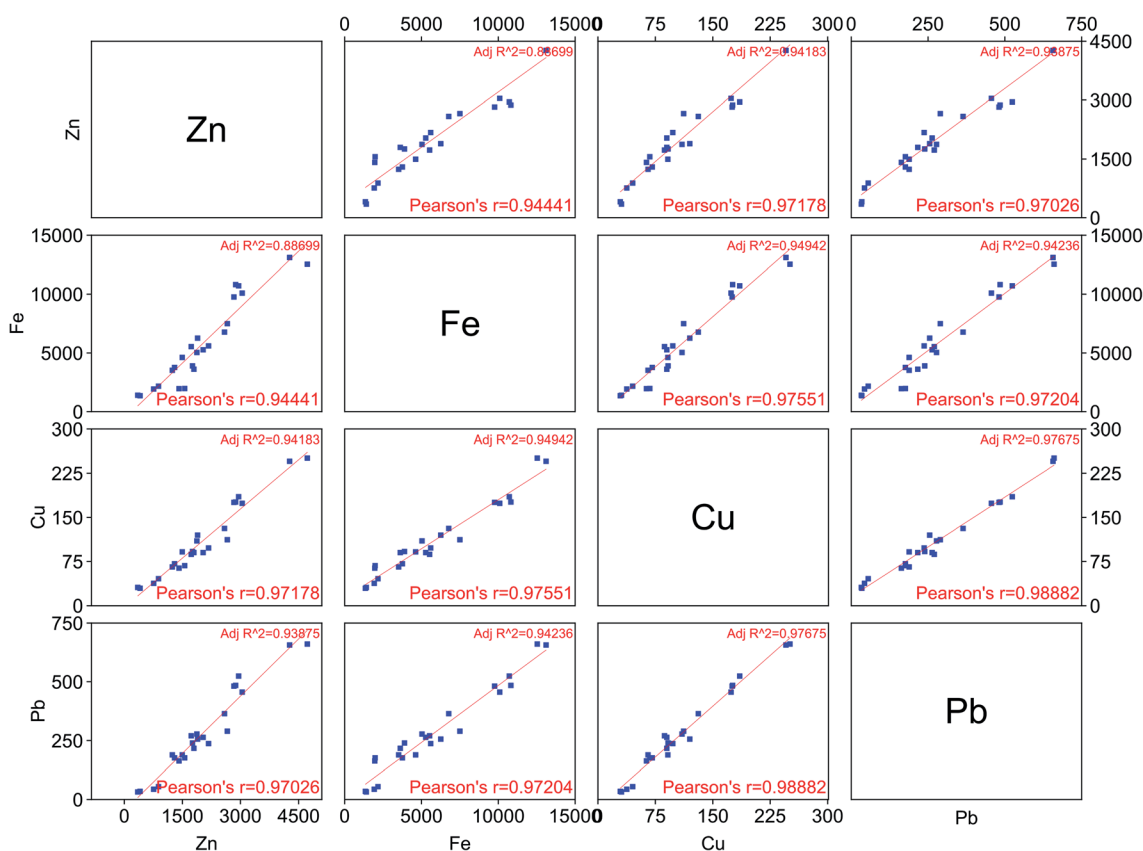


Fig. 7 Scatter plot for the composition of the pregnant leach solution (in ppm) using LevA-CaCl<sub>2</sub> ( $x_{\text{CaCl}_2} = 0.33$ ) and LevA-CaCl<sub>2</sub> ( $x_{\text{CaCl}_2} = 0.20$ ) under different experimental conditions.



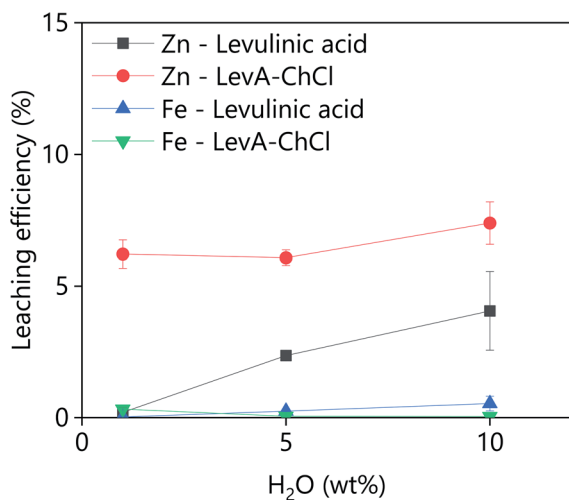


Fig. 8 Goethite leaching efficiency using LevA–ChCl ( $x_{\text{ChCl}} = 0.33$ ) and levulinic acid as a function of the water content.  $L/S = 10$ ;  $t = 2$  h;  $T = 30$  °C; 1000 rpm.

zinc was lower using pure levulinic than using the corresponding ChCl-based DES. Furthermore, pure levulinic acid was less selective against iron. From the obtained results it is concluded that the LevA–ChCl can leach more and more selectively than the individual components separately.

### Comparison with hydrometallurgical approaches

In order to critically assess the performance of LevA–ChCl for the valorisation of goethite, the leaching results were compared to those obtained using pure water and aqueous solutions of sulphuric acid ( $10 \text{ g L}^{-1}$  and  $80 \text{ g L}^{-1}$ ) as lixiviants. The selected concentrations correspond to the conditions used in the neutral and hot leaching of the RLE process for zinc production. The obtained results are compared in Fig. 9. Firstly, it has been verified that only a minor amount of metals can be leached using water, *i.e.*, the concentration of the metals in the pregnant leach solution was below  $25 \text{ mg L}^{-1}$ . This is expected because the residue is washed in the zinc plant. The goethite leaching using  $80 \text{ g L}^{-1}$  of sulphuric acid could dissolve up to 65 wt% of the zinc, but at the expense of a complete loss of selectivity against iron, *i.e.* the composition of the PLS was  $11\,800 \text{ mg L}^{-1}$  iron,  $3800 \text{ mg L}^{-1}$  zinc ( $\alpha = 0.32$ ). Decreasing the concentration of sulphuric acid to  $10 \text{ g L}^{-1}$  decreased the leaching efficiency of both zinc and iron, resulting in a selective process: the composition of the PLS is  $500 \text{ mg L}^{-1}$  iron,  $2300 \text{ mg L}^{-1}$  zinc ( $\alpha = 4.6$ ). Aqueous solutions of sulphuric acid can leach more copper and less lead than LevA–ChCl at any of the investigated conditions. For comparison, the leaching efficiency obtained using LevA–ChCl at two different conditions are also included in Fig. 9. These data correspond to the experiments in which the best selectivity while still relatively high leaching efficiency were achieved. In one of the experiments (denoted as DES leaching in Fig. 9), the leaching efficiency of zinc is slightly higher than in the neutral leaching, but less selective: the composition of the PLS was  $800 \text{ mg L}^{-1}$  iron,  $2800 \text{ mg L}^{-1}$  zinc ( $\alpha = 3.66$ ). In

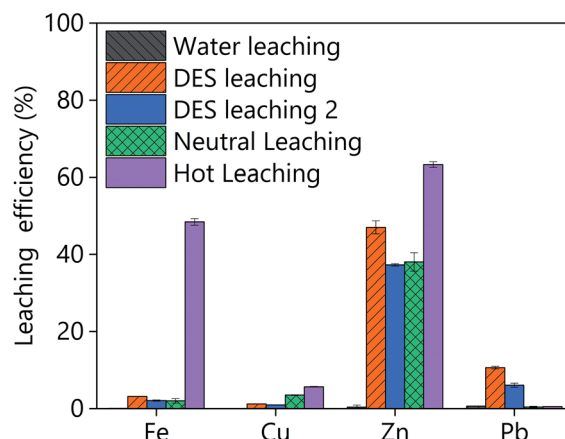


Fig. 9 Comparison of the leaching efficiencies of goethite using different lixiviants under the following conditions: water leaching:  $L/S = 10$ ,  $t = 2$  h,  $T = 40$  °C. DES leaching: LevA–ChCl;  $L/S = 10$ ,  $t = 2$  h,  $T = 40$  °C;  $\text{H}_2\text{O}$  (wt%) = 30. DES leaching 2: LevA–ChCl;  $L/S = 10$ ,  $t = 24$  h,  $T = 30$  °C,  $\text{H}_2\text{O}$  (wt%) = 30. Neutral leaching:  $\text{H}_2\text{SO}_4$   $10 \text{ g L}^{-1}$ ;  $L/S = 10$ ;  $t = 2.5$  h;  $T = 65$  °C. Hot leaching:  $\text{H}_2\text{SO}_4$   $80 \text{ g L}^{-1}$ ;  $L/S = 10$ ;  $t = 2$  h,  $T = 80$  °C.

another experiment (denoted as DES leaching 2 in Fig. 9), the obtained results are comparable to those of the neutral leaching: the composition of the PLS is  $500 \text{ mg L}^{-1}$  of iron,  $2200 \text{ mg L}^{-1}$  of zinc ( $\alpha = 4.4$ ). From this comparison it can be concluded that the performance of the DESs is not essentially better than that of the neutral leaching. Considering that sulphuric acid is produced *in situ* in the zinc plant at much lower price than the DES, the use of LevA–ChCl might not be justified for the selective recovery of zinc from the goethite residue. However, it was shown that the selective dissolution of metals is possible, and the obtained results might be of interest for other type of processes in which zinc is present in a more accessible form.

## Conclusions

In this work the leaching of goethite residue using DESs was investigated. An initial screening showed that carboxylic acid-based DESs can leach more metals than polyols and amides, and that quaternary phosphonium salts can leach more metals than quaternary ammonium salts. Levulinic acid–choline chloride was selected because of the best compromise between high zinc leaching efficiency and good selectivity against iron. Other DESs such as ethylene glycol–choline chloride are even more selective against iron, and its application could be further investigated. The water content of the DES and the leaching temperature have a big effect on the leaching efficiency whereas the leaching time on the selectivity against iron. Levulinic acid–choline chloride can leach more zinc more selectively than a mixture of levulinic acid and  $\text{CaCl}_2$  or than pure levulinic acid. Leaching with levulinic acid–choline chloride resulted in comparable selectivity and slightly higher zinc recovery compared to the conventional “neutral leaching” with  $10 \text{ g L}^{-1}$  sulphuric acid. Considering the high price of the DESs and the low profits that can be obtained from the valorisation of this



type of residues (low concentration of cheap based metals), the industrial implementation of this process is not attractive at this point. Economic penalties for stockpiling industrial residues might change the actual situation.

## Conflicts of interest

There are no conflicts to declare.

## Acknowledgements

The authors of this work acknowledge the Strategic Initiative Materials in Flanders (SIM) for the financial support (SBO-SMART: Sustainable Metal Extraction from Tailings) with grant no. HBC.2016.0456. Nerea Rodriguez Rodriguez acknowledges the financial support from the Research Foundation-Flanders (FWO, grant no. 12X5119N, postdoctoral fellowship). Nyrstar (Balen, Belgium) is gratefully acknowledged for providing the industrial process residue.

## References

- European Commission, *Connecting economic and environmental gains*, 2017.
- V. Moreau, M. Sahakian, P. van Griethuysen and F. Vuille, *J. Ind. Ecol.*, 2017, **21**, 497–506.
- B. Schwab, A. Ruh, J. Manthey and M. Drosik, in *Ullmann's Encyclopedia of Industrial Chemistry*, 2015.
- M. Pelino, C. Cantalini, C. Abbruzzese and P. Plescia, *Hydrometallurgy*, 1996, **40**, 25–35.
- B. Schwab, A. Ruh, J. Manthey and M. Drosik, Zinc, *Ullmann's Encyclopedia of Industrial Chemistry*, 2015, DOI: 10.1002/14356007.a28\_509.pub2.
- M. Pelino, C. Cantalini, P. P. Boattini, C. Abbruzzese, J. M. Rincon and J. E. Garcia Hernandez, *Resour. Conserv. Recycl.*, 1994, **10**, 171–176.
- M. Pelino, *Waste Manag.*, 2000, **20**, 561–568.
- J. F. Pusateri, C. O. Bounds and L. W. Lherbier, *JOM*, 1988, **40**, 31–35.
- S. Creedy, A. Glinin, R. Matusiewicz, S. Hughes and M. Reuter, *World Metall.-Erzmet.*, 2013, **66**, 230–235.
- J. Hoang, M. A. Reuter, R. Matusiewicz, S. Hughes and N. Piret, *Miner. Eng.*, 2009, **22**, 742–751.
- L. Piga, L. Stoppa and R. Massidda, *Resour. Conserv. Recycl.*, 1995, **14**, 11–20.
- K. Verscheure, M. Van Camp, B. Blanpain, P. Wollants, P. Hayes and E. Jak, *Metall. Mater. Trans. B*, 2007, **38**, 13–20.
- A. Di Maria and K. Van Acker, *Engineering*, 2018, **4**, 421–429.
- E. Ntumba Malenga, A. F. Mulaba-Bafubandi and W. Nheta, *Hydrometallurgy*, 2015, **155**, 69–78.
- H. Han, W. Sun, Y. Hu, B. Jia and H. Tang, *J. Hazard. Mater.*, 2014, **278**, 49–54.
- A. Ruşen, A. S. Sunkar and Y. A. Topkaya, *Hydrometallurgy*, 2008, **93**, 45–50.
- P. Asokan, M. Saxena and S. R. Asolekar, *J. Hazard. Mater.*, 2006, **137**, 1589–1599.
- P. Asokan, M. Saxena and S. R. Asolekar, *Mater. Charact.*, 2010, **61**, 1342–1355.
- S. Ju, Y. Zhang, Y. Zhang, P. Xue and Y. Wang, *J. Hazard. Mater.*, 2011, **192**, 554–558.
- S. Van Roosendael, M. Regadio, J. Roosen and K. Binnemans, *Sep. Purif. Technol.*, 2019, **212**, 843–853.
- K. Binnemans and P. T. Jones, *J. Sustain. Metall.*, 2017, **3**, 570–600.
- T. Palden, B. Onghena, M. Regadio and K. Binnemans, *Green Chem.*, 2019, **21**, 5394–5404.
- T. Palden, M. Regadio, B. Onghena and K. Binnemans, *ACS Sustain. Chem. Eng.*, 2019, **7**, 4239–4246.
- F. Forte, L. Horckmans, K. Broos, E. Kim, F. Kukurugya and K. Binnemans, *RSC Adv*, 2017, **7**, 49999–50005.
- S. Riaño, M. Petranikova, B. Onghena, T. Vander Hoogerstraete, D. Banerjee, M. R. S. Foreman, C. Ekberg and K. Binnemans, *RSC Adv*, 2017, **7**, 32100–32113.
- L. Gijsemans, F. Forte, B. Onghena and K. Binnemans, *RSC Adv*, 2018, **8**, 26349–26355.
- M. A. R. Martins, S. P. Pinho and J. A. P. Coutinho, *J. Solution Chem.*, 2019, **48**, 962–982.
- A. P. Abbott, G. Capper, D. L. Davies, R. K. Rasheed and V. Tambyrajah, *Chem. Commun.*, 2003, 70–71.
- E. L. Smith, A. P. Abbott and K. S. Ryder, *Chem. Rev.*, 2014, **114**, 11060–11082.
- A. P. Abbott, G. Capper, D. L. Davies, K. J. McKenzie and S. U. Obi, *J. Chem. Eng. Data*, 2006, **51**, 1280–1282.
- A. P. Abbott, G. Capper, D. L. Davies, R. K. Rasheed and P. Shikotra, *Inorg. Chem.*, 2005, **44**, 6497–6499.
- N. Rodriguez Rodriguez, L. Machiels and K. Binnemans, *ACS Sustain. Chem. Eng.*, 2019, **7**, 3940–3948.
- A. P. Abbott, J. Collins, I. Dalrymple, R. C. Harris, R. Mistry, F. Qiu, J. Scheirer and W. R. Wise, *Aust. J. Chem.*, 2009, **62**, 341–347.
- M. Regadio, S. Riaño, K. Binnemans and T. Vander Hoogerstraete, *Anal. Chem.*, 2017, **89**, 4595.
- C. Florindo, F. S. Oliveira, L. P. N. Rebelo, A. M. Fernandes and I. M. Marrucho, *ACS Sustain. Chem. Eng.*, 2014, **2**, 2416–2425.
- M. Gräfe, M. Landers, R. Tapper, P. Austin, B. Gan, A. Grabsch and C. Klauber, *J. Environ. Qual.*, 2011, **40**, 767–783.
- T. Yang, Z. Zhu, Y. Wu and Z. Rao, *Environ. Geol.*, 2008, **56**, 309–316.

